Chapter 4

Analysis of radiation transport through multileaf collimators using Monte Carlo Simulations

ABSTRACT

The Monte Carlo simulations are established as most reliable and accurate methods for the analysis of radiation beam properties. The work present in this chapter demonstrate a practical means of determining the properties of radiation beam as it is being transported through the multileaf collimators(MLC) which are part of secondary collimators system (tertiary collimators as attachment) and are the key elements used for delivery of modern radiotherapy treatments . In dynamic IMRT treatment delivery, relatively increased numbers of monitor units are used due to which the total MLC leakage can exceed up to 10% of the maximum in-field dose. To avoid these dosimetric errors, the MLC leakage must be accurately accounted for; in the dose calculation and conversion of optimized intensity patterns to MLC trajectories used for treatment delivery. In this study, we have used the BEAMnrc Monte Carlo code system to investigate the characteristics of radiation transported through the multileaf collimators for 6 MV photon beam produced by Varian linear accelerator. Accurate simulation model of Varian Clinic 600 unique performance was made to calculate MLC radiation leakage as a function of field size by precisely modelling the complex geometry of 120-leaf Varian Millennium^{TM} Multileaf Collimators. We have also evaluated the effect of MLC on percentage depth dose characteristics, photon spectra and photon average energy distributions. A significant increase in MLC leakage with increase in field size was observed in our study. Photon spectra and photon average energy distributions were found to be substantially modified by MLC as it removes lower-energy photons resulting in increase of PDDs for MLC blocked fields in comparison to the jaw define open fields.

4.1 INTRODUCTION

The planning aspect of intensity modulated radiation therapy (IMRT) treatment delivery relies on the use of multileaf collimators (MLC) to produce the desired intensity pattern. Standard MLC, originally were developed to replace the metal alloy blocks, are now used for delivering IMRT treatments with different methods. Examples of these different methods include step-and-shoot beam delivery **[Bortfeld *et al.* (1994), Galvin *et al.* (1993), Fraass *et al.* (1999), Xia *et al.* (1998)],** dynamic-MLC (DMLC) beam delivery **[Kallman *et al.* (1988), Convery *et al.* (1992), Gustafsson *et al.* (1995), Spirou *et al.* (1994), Yu (1995), Svensson *et al.* (1994), Stein *et al.* (1994)],** and intensity modulated arc therapy (IMAT) **[Yu *et al.* (1995)]**.The complex intensity pattern used to deliver the desired dose distributions of the above mention treatments are very sensitive to the detailed structure of MLC. In an IMRT treatment to treat the desire section of a treatment field rest portion is blocked by MLC. In these blocked segments significant portion of dose can be delivered due to radiation leakage from MLC. The contribution of MLC leakage to a point in an IMRT field can be calculated by the static field leakage multiplied by the product of the number of monitor units delivered for the IMRT field and the fraction of time the point is blocked by the MLC. Dependency of MLC leakage radiation on these factors and increment in its value consequently has been reported in literature [**Mohan *et al*. (2000)].** Previously in a Monte Carlo (MC) study an increase in MLC leakage value with increase in field size has been reported **[Kim *et al*. (2001)]**. Thus the undesired dose delivered due to leakage radiation from MLC must be considered in entire dose calculation procedure and in the conversion from optimized intensity patterns to MLC trajectories used for treatment delivery to avoid any dosimetric errors. The Monte Carlo methods have been used extensively to estimate accurate dose
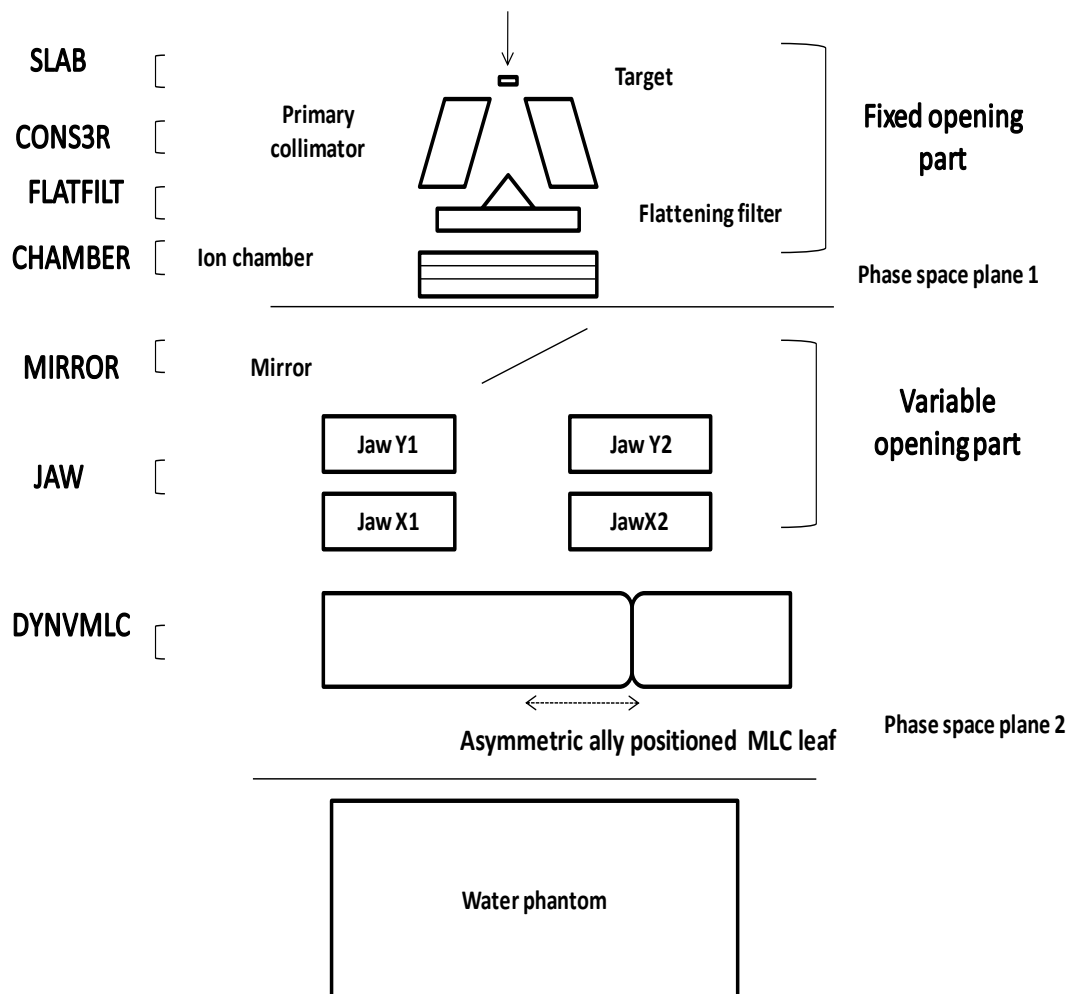
distributions for clinical beams. Several studies have been conducted using these methods for analyzing influence of linac head components on beam characteristics **[Verhaegen *et al*. (2003), Sheikh-Bagheri *et al*. (2002), Mesbahi *et al*. (2006)]**. Studies describing the beam hardening effect of flattening filter on photon energy spectra, absorbed dose and beam profiles have also been published **[Lee *et al* (1997)]**. Therefore, Monte Carlo simulation model can be used to accurately calculate the effect of MLC on dose distributions for a typical modern accelerator such as Varian Clinic 600 unique performance. Our study reports on variation of radiation leakage from MLC as a function of field size for 120- leaf Varian MillenniumTM Multileaf Collimator. We have also calculated the effect of MLC on percentage depth dose characteristics, photon spectra and photon average energy distributions. The effect of using MLC to define treatment field on surface dose and electron fluence spectra have also being evaluated in our study.

4.2 Material & Methods

In this study we developed the simulation model of Varian Clinic 600 unique performance linear accelerator using BEAMnrc code System. The entire geometry and materials used to build the MC simulation model of the linear accelerator were based on the machine specifications as provided by the manufacturer Varian Medical Systems. The linac structure was ordered as: a target slab of tungsten and copper, primary collimator (tungsten), flattening filter, ion chamber, mirror, jaws (tungsten) and finally the option for 120- leaf Varian Millennium^{TM} Multileaf Collimator. To model the geometry of 120-leaf Varian Millennium^{TM} Multileaf Collimator special geometry package of BEAMnrc was used. The 120-leaf MLC consists of two banks of 60 leaves each. The 40 central leaves produce a 0.5 cm resolution at 100 cm source to surface distance (SSD) and the 20 outer leaves produce a

1.0 cm resolution at 100 cm SSD. All details of the leaf design were included in the Monte Carlo geometry, including the tongue-and-groove used to reduce radiation leakage through interfaces between adjacent leaves and the complex rounded leaf tip. All materials used in the Monte Carlo (MC) simulation were extracted from the 700 ICRU PEGS4 (pre-processor for Electron Gamma Shower) cross section data available in BEAMnrc, and met the specifications for the linac as provided by the manufacturer. Different stages of simulation and component module used to model various component of 6 MV photon beam produced by Varian Linac using principal features of BEAMnrc-DOSXYZnrc code are shown in figure 4.1. Initially $1 \cdot 5 \times 10^8$ histories were used, a monoenergetic electron beam source of kinetic energy of $5 \cdot 7$ MeV with a full width at half maximum (FWHM) for the X and Y directions of $0 \cdot 2$ cm was made to strike the target. The primary collimator, flattening filter and ion chamber were included in this step. This step results in a phase space file on the first scoring plane as shown in figure 4.1 containing detailed information of all the particles reaching this plane and there after exiting downstream from the end of ion chamber. This phase space data was reused for the next step of simulation for simulating the particle transport through secondary collimator systems defining different field sizes. The second step of the calculation simulates the passage of the particles through the mirror; adjustable collimators, MLC and air slab to a plane at SSD 100 cm from target. We simulated different openings of jaw as well as MLC to get field sizes from 5×5 to 20×20 cm^2 at an SSD equal to 100 cm. For the latter case in MLC define field sizes the projected jaws (X & Y) setting was 5 cm larger than that of MLC. In addition for MLC leakage calculations, MLC leaves were configured to fully block the open field produced by the jaw with the leaves of MLC were positioned asymmetrically with respect to the central axis. The output of this step is a phase space file at plane two as show in figure 4.1. The data analysis program BEAMDP was used to analyze the phase space data files to extract the various types of spectra of all particles reaching the plane at SSD 100

cm. The effect of MLC on photon beam characteristics was determined by calculating and comparing the photon spectra on central axis and average energy distributions at 100 cm SSD for a jaw-defined open field and the same field blocked by the MLC for various field sizes. Photon interactions within the MLC can generate secondary electrons that can contribute dose to a patient. To determine the relative dose contributions from these secondary electrons, electron spectra for MLC define and jaw define field size were also calculated in our study. In the third step of simulation these phase space file obtained for different field sizes defined by different elements of secondary collimator system were imported as an input inside a water phantom created in DOSXYZnrc code as shown in figure 4.1 for the dose calculations. The water phantom used for the dose calculation was of dimension $30 \times 30 \times 30$ cm^3 with a voxels size of $0 \cdot 25 \times 0 \cdot 25 \times 0 \cdot 25$ cm^3. We used our simulation model to calculate percentage depth dose curves (PDDs) for MLC blocked field which were compared with PDDs of jaw define open field to illustrate the effect of MLC on depth dose characteristics. In addition the surface dose were evaluated and compared for jaw and MLC define fields in this study.

SLAB [

CONS3R [

FLATFILT [

CHAMBER [Ion chamber

Primary
collimator

Target

Flattening filter

Fixed opening
part

Phase space plane 1

MIRROR [Mirror

JAW [

Jaw Y1   Jaw Y2

Jaw X1   Jaw X2

Variable
opening part

DYNVMLC [

Asymmetric ally positioned MLC leaf

Phase space plane 2

Water phantom

Figure 4.1 Simulation model for Varian Linac split into three parts: treatment head fixed
Opening part up to scoring plane one, Variable opening part between Scoring
Plane one and two with MLC leaf positioned asymmetrically and dose calculation
Inside the water phantom .

4.3 MLC leakage Calculations: MLC leakage is an important parameter needed for the

commissioning of a treatment-planning system. We have calculated the MLC leakage as a

function of field size in our study which is presented in table 4.1. MLC leakage represents the

dose on the central beam axis with MLC blocked fields normalized by the dose of jaw define

open fields of the same field size at 1.5 cm depth for SSD 100 cm. Jaw defined open field are

those in which the MLC leaves are withdrawn underneath the jaws and the field size is

defined by the treatment jaws only. MLC blocked fields are defined as a field in which the

MLC leaves are configured to fully block the open field produced by the jaw. To ensure that the jaws blocked the rounded tips of the leaves completely in MLC blocked fields, the leaves of MLC were positioned asymmetrically with respect to the central axis and their projected offset was 8.0 cm from isocenter as shown in figure 4.1.
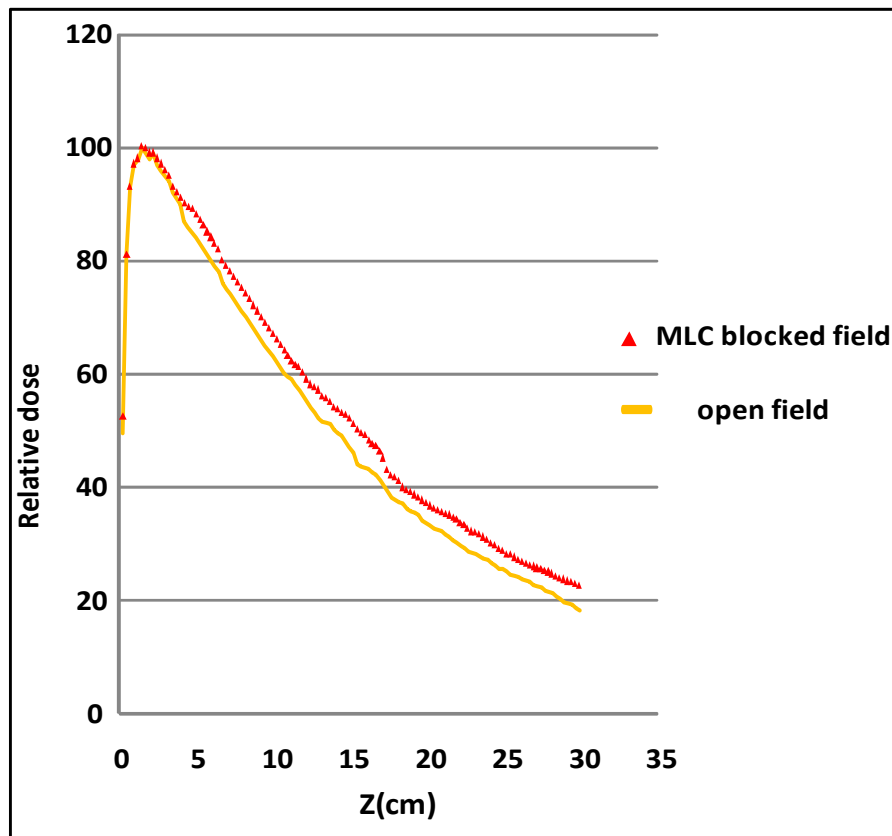
Table 4.1 MLC leakage calculated for 6 MV photon beam for different field sizes. Abbreviations: Calculation was made at 1.5 cm depth and SSD 100 cm.

| Field size A (cm^2)	MLC leakage (%)
5×5	1.20
10×10	1.40
15×15	1.57
20×20	1.72

4.4 Percentage depth-dose characteristics

Percentage depth-dose characteristics were calculated in our study for both MLC blocked and jaw define open fields for different field sizes. It can be seen from figure 4.2 that MLC blocked beam show slightly higher PDDs values in comparison to the jaw defined open beam for all field sizes. Difference in the PDDs between the two cases is evident at deeper depths and is increased with increase in depth for all field sizes. This difference is validated by calculating the two parameters which are reported in table 4.2, namely, the relative dose at a depth of 10 and 20 cm (D_{10}, D_{20}). Our results are in good agreement with the results reported by **Kim *et al*. [Kim *et al*. (2001)**, in which they coated an increase in PDDs for MLC blocked field in comparison to open field.

(a)
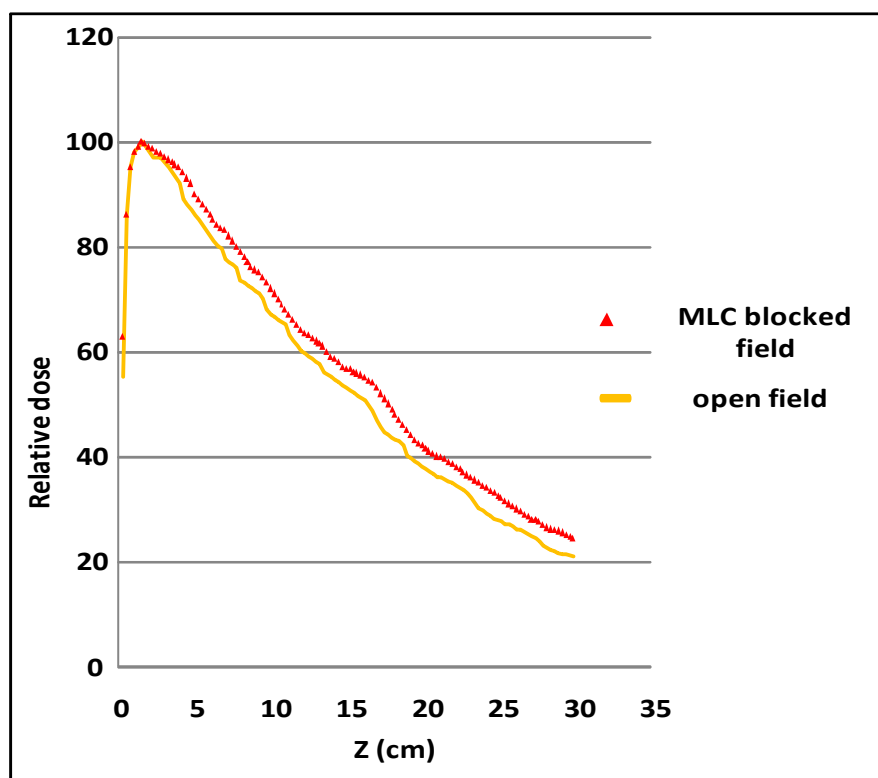
(b)

Figure 4.2 Comparison of relative depth dose curves calculated for MLC blocked and jaw define open fields for 6MV photon beams for a field size of **(a)** 10×10 cm^2 **(b)** 20×20 cm^2

Table 4.2 Comparison of relative depth doses for MLC blocked and jaw define Open fields at two reference depths for different field sizes. Abbreviations: A denotes the field size; D$_{10}$ and D$_{20}$ denotes relative depth dose at 10 and 20 cm depth

| Field size A (cm^2) | Relative depth doses | | | |
| | D$_{10}$ | | D$_{20}$ | |
	MLC blocked fields	jaw define open fields	MLC blocked fields	jaw define open fields
5×5	68.0	61.87	39.8	33.14
10×10	69.8	66.67	41.15	37.32
15×15	70.12	66.83	42.6	39.2
20×20	73.10	67.57	47.23	41.6

4.5 Analysis of Spectra

4.5.1 Photon fluences spectra

Figure 4.3 shows central axis photon spectra as a function of energy (number of photons per MeV per incident electron on the target) for both MLC blocked and jaw define open fields for 20×20 cm^2 field size. Photon originated in target passes through the collimating system on their way to the scoring plain at an SSD 100 cm. Scoring plain is an annular region around

the central axis with radius of 2.25 cm. The range of possible energy of photon is divided into interval (bin) of 0.25 MeV. The number of photon within each energy bin crossing the scoring plain is being recorded separately for both MLC blocked and jaw define open fields. In figure 4.3 for comparison, the fluence plots are normalized in such a way that total area under each curve is equals to one. The precision of calculated central-axis photon spectra is high and uncertainty in each 0.25 MeV wide bin is usually between 1 to 5%, except for the high-energy end of the spectra. It was observed from figure 4.3 that for MLC blocked field the fluence of photon were having more high energy photons in comparison to the jaw define open field. Our results are in agreement with the results reported by **Kim *et al*. [Kim *et al*. (2001)]**, in which they coated an harder photon spectra for MLC blocked field in comparison to open field.
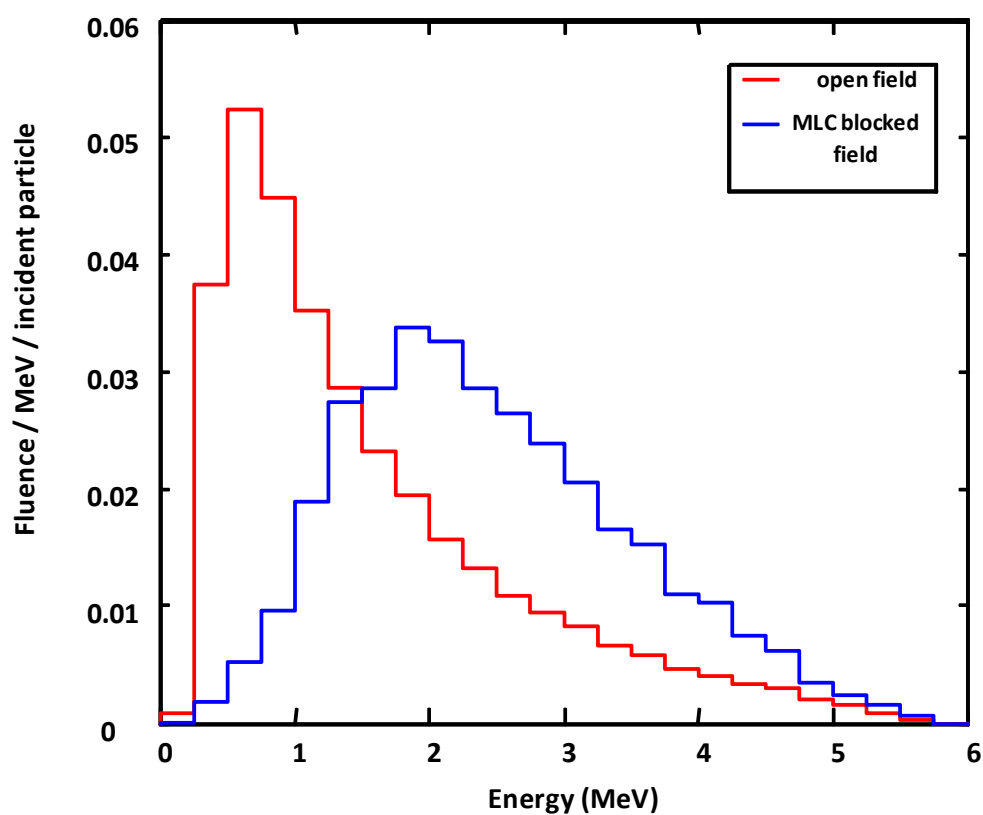
Figure 4.3 Photon fluences per initial electron on the target, at the top of the water phantom as a function of energy (MeV) for field size 20×20 cm^2 .

4.5.2 Average energy distribution

Photon average energy distribution as a function of off axis distance for field size 20×20 cm^2 at 100 cm SSD was calculated in our study for both MLC blocked and jaw define open fields. Considerable differences in average energy distribution for the two cases were observed which are presented in figure 4.4. It was observed from above distribution that mean photon energy for MLC blocked beam was 2.5 MeV at central axis which decreased to 1.56 MeV for jaw define open fields. This decrease in mean energy demonstrated the beam hardening effect produced by the MLC for photon beam.
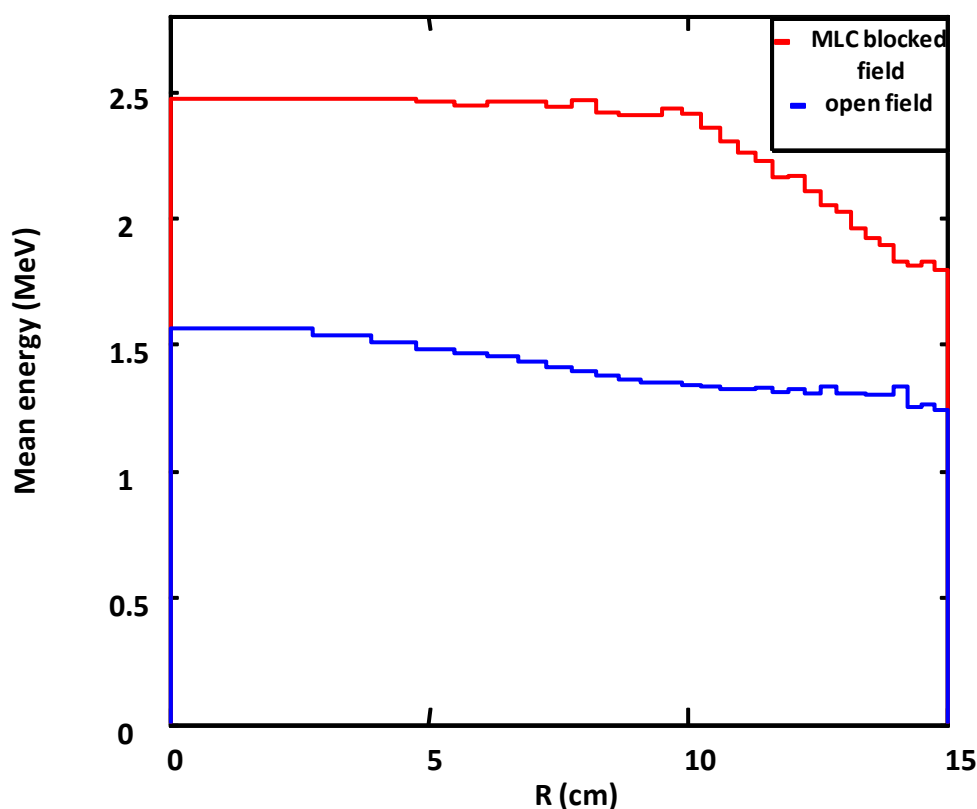
Figure 4.4 Photon average energy distribution for the MLC blocked and jaw define open fields as a function of off axis distance for a field size of 20×20 cm^2 and SSD of 100 cm.

4.5.3 Electron fluence spectra

Increase in electron fluence can causes the risk of placing ion chamber used for the measurement outside the range of its reliable operation. Also, it is a major component of elevated skin dose delivered to patient. Figure 4.5 shows the calculated electron fluence spectra as a function of off axis distance for 20×20 cm^2 field size at 100 cm SSD for both MLC and jaw define fields. In our study, it was found that the fluence of electron reaching the phantom surface increases for MLC define fields in comparison to jaw define fields. It was observed from above fluence spectra that the fluence at the centre for MLC define field was 1.23 times greater than its value for jaw define field.
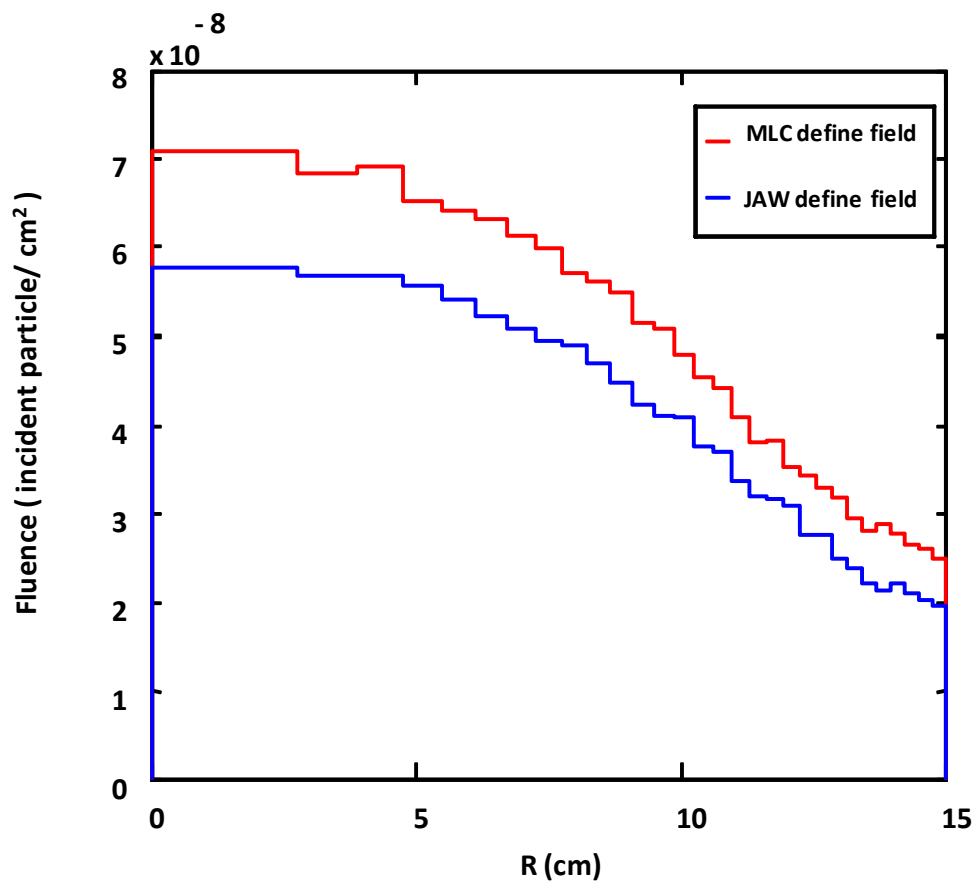
Figure 4.5 Electron fluences per initial electron on target, at the top of the water phantom as a function of off axis distance for 20×20 cm^2 field size calculated for both MLC and Jaw define field.

4.6 Surface Dose

Surface dose has been calculated for different field sizes for both MLC and jaw define fields and is presented in table 4.3. The PDD of first scoring voxels with 0.25 cm thickness from the top of water phantom surface was taken as a measure of surface dose. There were differences in doses of build up region between MLC and jaw defines fields. Surface dose was affected significantly by contaminant electrons reaching the phantom surface and due to higher fluence of electron for MLC define beam and the surface dose was found to be higher in comparison to jaw defined fields.

Table 4.3 Surface doses for MLC and jaw define fields for different field sizes.

Field size (cm^2)	Surface dose (jaw define field)	Surface dose (MLC define field)
5×5	47.80	49.43
10×10	49.40	52.32
15×15	53.20	57.39
20×20	55.19	62.88

4.7 Discussion & conclusions

In the present chapter our investigation was focused upon evaluating the properties of radiation beam as it is being transported through the secondary collimators system consisting of multileaf collimators which are used to deliver inhomogeneous fluence required for many morden radiotherapy treatments. To carry out this task, we performed Monte Carlo simulations to investigate how the various characteristics of photon beam including changes

in spectrum are affected by the MLC. We used our simulation model to calculate MLC leakage as a function of field size. It was observed that the calculated MLC leakage value increases with increase in field size. Our results were found to be in agreement with those reported by **Kim *et al*. [Kim *et al*. (2001)]**, in which they stated an increase in MLC leakage value with increase in field size. The calculated PDDs for MLC blocked field showed slightly higher values in comparison to the jaw define open beam for all field sizes. Differences in the PDDs between the two cases were found to increase with increase in depth for all field sizes. In our study we calculated average energy distribution of photon as a function of off axis distance and central axis photon fluence spectra as a function of energy for both MLC blocked and jaw define open fields for 20×20 cm^2 field size. Significant increase in average energy on central axis was observed for MLC blocked field in comparison to jaw define open field. This increment in average energy is due to the removal of low energy photons by MLC which also affects the on axis photon spectra as for MLC blocked field it contains more high energy photons in comparison to the jaw define open field. The results obtained in our study showed that the MLC substantially modified the photon energy spectrum of radiation beam by removing the lower-energy photons which results in rise of PDDs for MLC blocked fields in comparison to the jaw define open fields for all field sizes. In our study we calculated surface dose for both MLC and jaw define fields. Clear increment in surface dose for MLC define fields was observed. These results were further verified with the calculation of electron fluence spectra as a function of off axis distance for 20×20 cm^2 field size at 100 cm SSD for both MLC and jaw define fields. Considerable increase in electron fluence was observed for MLC define fields in comparison to jaw define fields. The possible explanation for this increment is that the use of MLC to define treatment field increases the photon interactions within the MLC which causes generation of secondary electrons. These low energy electrons contribute to surface dose.